Available online at www.sciencedirect.com
SCIENCE DIRECT
Carbohydrate Research 341 (2006) 1020–1028
Carbohydrate RESEARCH

# Molecular dynamics simulations of trehalose as a 'dynamic reducer' for solvent water molecules in the hydration shell

Youngjin Choi,[a] Kum Won Cho,[b] Karpjoo Jeong[c,*] and Seunho Jung[d,*]

[a]*Bio/Molecular Informatics Center, Konkuk University, Seoul 143-701, Republic of Korea*
[b]*Korea Institute of Science and Technology Information, Daejeon 305-806, Republic of Korea*
[c]*College of Information and Communication and Department of Advanced Technology Fusion, Konkuk University, Seoul 143-701, Republic of Korea*
[d]*Department of Microbial Engineering and Department of Bioscience and Biotechnology, Konkuk University, 1 Hwayang-dong Gwangjin-gu, Seoul 143-701, Republic of Korea*

Received 8 November 2005; received in revised form 11 February 2006; accepted 21 February 2006
Available online 20 March 2006

**Abstract**—Systematic computational work for a series of 13 disaccharides was performed to provide an atomic-level insight of unique biochemical role of the α,α-(1→1)-linked glucopyranoside dimer over the other glycosidically linked sugars. Superior osmotic and cryoprotective abilities of trehalose were explained on the basis of conformational and hydration characteristics of the trehalose molecule. Analyses of the hydration number and radial distribution function of solvent water molecules showed that there was very little hydration adjacent to the glycosidic oxygen of trehalose and that the dynamic conformation of trehalose was less flexible than any of the other sugars due to this anisotropic hydration. The remarkable conformational rigidity that allowed trehalose to act as a sugar template was required for stable interactions with hydrogen-bonded water molecules. Trehalose made an average of 2.8 long-lived hydrogen bonds per each MD step, which was much larger than the average of 2.1 for the other sugars. The stable hydrogen-bond network is derived from the formation of long-lived water bridges at the expense of decreasing the dynamics of the water molecules. Evidence for this dynamic reduction of water by trehalose was also established based on each of the lowest translational diffusion coefficients and the lowest intermolecular coulombic energy of the water molecules around trehalose. Overall results indicate that trehalose functions as a 'dynamic reducer' for solvent water molecules based on its anisotropic hydration and conformational rigidity, suggesting that macroscopic solvent properties could be modulated by changes in the type of glycosidic linkages in sugar molecules.
© 2006 Elsevier Ltd. All rights reserved.

*Keywords:* Molecular dynamics simulations; Anisotropic hydration; Conformational flexibility; Disaccharide; Glycosidic linkage; Long-lived hydrogen bond

## 1. Introduction

Trehalose (α-D-glucopyranosyl-(1→1)-α-D-glucopyranoside) is a fully symmetrical disaccharide of glucose linked through an α,α-(1→1)-glycosidic bond. It is one of the most chemically stable sugars in nature and has many useful biological applications.[1] It serves as a bioprotector for living organisms against environmental stresses including extreme dehydration, freezing, oxidation, and hyperosmotic pressure.[2] The biosynthesis of trehalose is a highly energy-consuming process that involves the transfer of glucose from UDP glucose to glucose-6-phosphate to produce trehalose-6-phosphate.[3] An alternative pathway that has been recently reported in some bacteria converts an α,α-(1→4)-linked glucose polymer (i.e., starch) to the α,α-(1→1)-glycosidic linkage of trehalose.[4] Trehalose, in particular, is also known to

* Corresponding authors. Tel.: +82 2 450 3520; fax: +82 2 452 3611; e-mail addresses: jeongk@konkuk.ac.kr; shjung@konkuk.ac.kr

0008-6215/$ - see front matter © 2006 Elsevier Ltd. All rights reserved.
doi:10.1016/j.carres.2006.02.032

be a compatible solute found in various Gram-negative rhizosphere bacteria such as those of the *Rhizobium*, *Azospirillum*, and *Pseudomonas* genera.[5] Bacterial cells respond to extracellular osmotic pressure by modulating their cytoplasmic water activity upon a synthesis of compatible solutes. Trehalose effectively prevents water flows across cellular membranes caused by gradients of water activity.

Such important biological roles of trehalose have been found in a variety of bacterial strains by many research groups. But theoretical studies on the main factor in determining the osmo- or cryoprotective activity of trehalose have not yet been fully carried out. Several researchers have pointed out that the highest glass-transition temperature of trehalose may contribute to the preservation of biological molecules through the control of water mobility.[6] The direct interaction of trehalose with lipid head groups by 'water replacement' has also suggested this as a protection mechanism for biomembrane stabilization.[7] The order of glass-transition temperatures by Green et al.,[8] trehalose > maltose > sucrose > glycerol, coincides with the order found by Crowe et al.[6] for the efficiency of membrane preservation upon dehydration at low water activity.

Recent computational work on the conformation of trehalose indicated that the less flexible α,α-(1→1)-glycosidic linkage of trehalose could be an important clue to explain its biological functions.[9] Liu et al.[10] found from their molecular dynamics results that the anisotropic hydration of trehalose with its rigid conformation may be related to the specific biological role of trehalose in the aqueous environment. However, they could not give a clear reason as to why trehalose can be more effective in controlling neighboring water molecules than other sugars.

There have been a number of efforts to find interrelationships between water of hydration and biomolecular conformation, including carbohydrates. X-ray, neutron scattering, and NMR dispersion techniques are the representative experimental methods that satisfy such purposes.[11] Magazù and co-workers have studied the transport properties of trehalose, maltose, and sucrose in $D_2O$ solution.[12] They obtained the self-diffusion coefficient of disaccharide ($D$) and the apparent diffusion coefficient ($D_{app}$) by means of $^1H$ pulse-gradient-spin-echo NMR (PGSE-NMR) and quasi-elastic light-scattering (QELS) techniques. The interpretation of the concentration dependence of $D$ and $D_{app}$ by means of a rigid spheres model has been successfully tested on trehalose and sucrose solutions. Kawai et al.[13] and Magazù et al.[14] showed by NMR and ultrasonic measurements that trehalose has a very high ability to bind water. These authors found also that at high concentrations the two rings of the disaccharide should somehow overfold, forming intermolecular hydrogen-bridged bonds, a fact that was confirmed by Elias and Elias.[15]

However, it is impossible to enumerate the number of hydration waters or to define specific hydration sites of the sugar or biomolecules.[16] Furthermore, a study of water dynamics near the sugar molecules is limited by highly averaged information obtained over an inhomogeneous sugar surface in various conformational states. Thus, it is highly desirable to investigate the hydrational water dynamics of the solvated sugar system using a computer-aided simulation method. Pérez and co-workers studied the hydrational pattern of trehalose solution with the CHARMM force field.[17] Pablo's group estimated the diffusion coefficient of a sugar solution with the OPLS force field.[18] In the present work, systematic molecular dynamics (MD) simulations have been performed to find a theoretical reason as to why nature selected trehalose as a bioprotectant over a series of other disaccharides. A total of 13 different homodisaccharides of gluco-(Glc*p*), galacto-(Gal*p*), or mannopyranose (Man*p*) with different glycosidic linkages were examined as in the flowing: α-D-Glc*p*-(1→1)-α-D-Glc*p* (**1**, trehalose), β-D-Glc*p*-(1→1)-β-D-Glc*p* (**2**, isotrehalose), α-D-Glc*p*-(1→1)-β-D-Glc*p* (**3**, neotrehalose), α-D-Glc*p*-(1→2)-α-D-Glc*p* (**4**, kojibiose), α-D-Glc*p*-(1→3)-α-D-Glc*p* (**5**, nigerose), α-D-Glc*p*-(1→4)-α-D-Glc*p* (**6**, maltose), α-D-Glc*p*-(1→6)-α-D-Glc*p* (**7**, isomaltose), β-D-Glc*p*-(1→2)-β-D-Glc*p* (**8**, sophorose), β-D-Glc*p*-(1→3)-β-D-Glc*p* (**9**, larminarabiose), β-D-Glc*p*-(1→4)-β-D-Glc*p* (**10**, cellobiose), β-D-Glc*p*-(1→6)-β-D-Glc*p* (**11**, gentiobiose), α-D-Gal*p*-(1→1)-α-D-Gal*p* (**12**), and α-D-Man*p*-(1→1)-α-D-Man*p* (**13**). The stable solution conformations for each disaccharide were traced with 10-ns molecular dynamics simulations using the CHARMM[19] program with revised carbohydrate force field[20] for aqueous MD simulations. We found that the long-lived hydrogen bonds with water and conformational rigidity caused by anisotropic hydration of trehalose were responsible for a 'dynamic reducer' function of trehalose on the solvent water molecules over the effects seen for other sugars. Our goal is to clarify the relationship between the hydration pattern of carbohydrates and the biological function at an atomic level throughout molecular dynamics simulations.

## 2. Computational methods

Molecular models for each disaccharide were built with the InsightII/Biopolymer program (version 2000, Accelrys Inc. San Diego, USA). The glycosidic linkage -(1→X)- in every sugar is described by two dihedral angles: $\varphi$ = H-1–C-1–O-1–C-X and $\psi$ = C-1–O-1–C-X–H-X. Their two-dimensional molecular schemes are presented in Figure 1.

The initial coordinates of each disaccharide were obtained from the GlycoSciences Database (http://www.glycosciences.de/). The geometries of these molecular

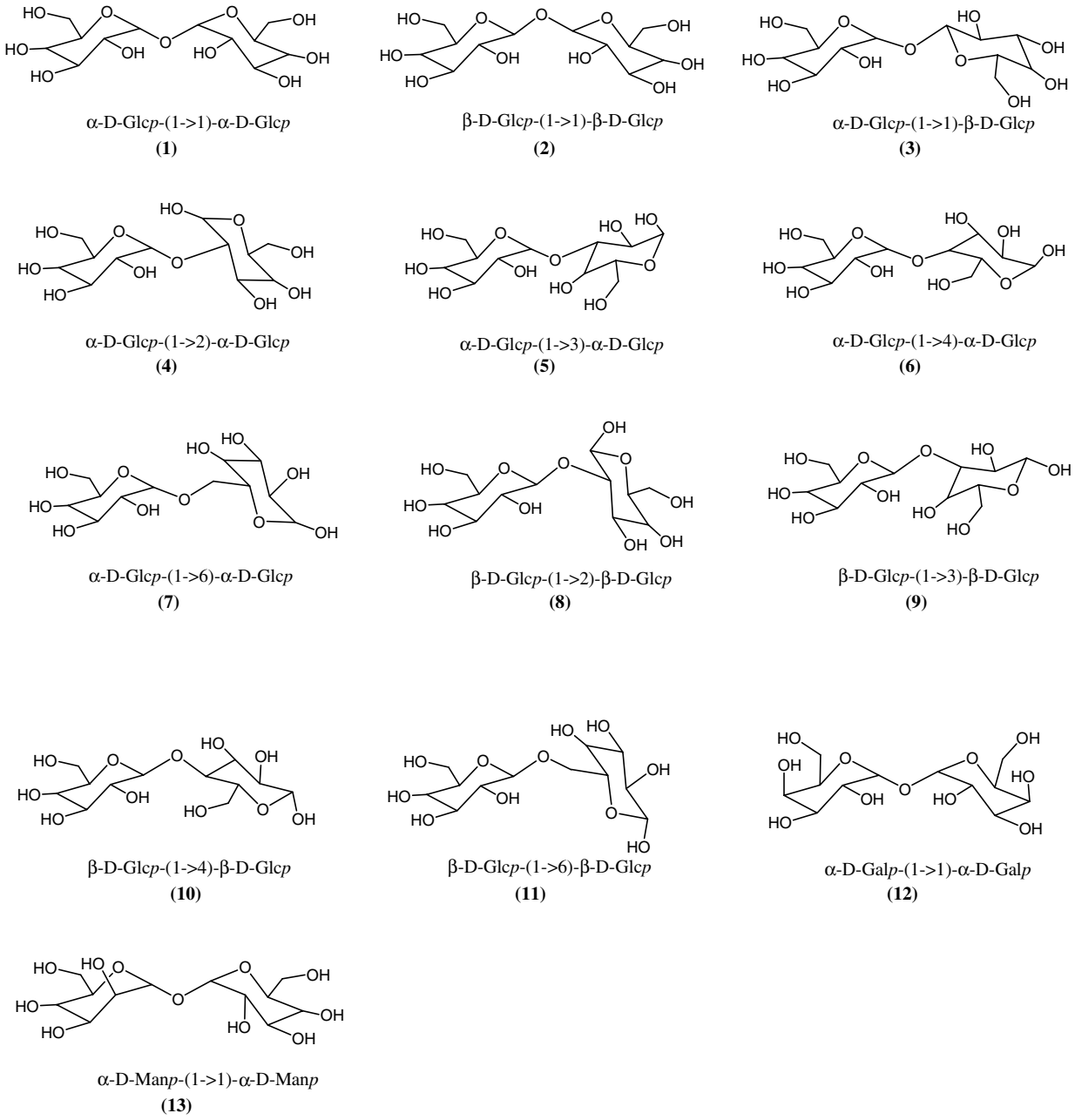


**Figure 1.** Schematic diagrams of the glycosidic linkage model of the sugars studied in this work.

models were fully optimized before MD runs. A TIP3P three-site rigid water[21] model was used to solvate each sugar. Water molecules were removed if they were closer than 2.8 Å to any heavy atoms of the sugars. In summary, each system was constructed using periodic boundary conditions with a cubic box of dimensions 25 Å × 25 Å × 25 Å, consisting of the sugar–water molecules. Final concentrations of each sugar solution were approximately 4% (w/w). The system was minimized by 1000 steps of conjugate gradient, followed by Adopted Basis Newton–Raphson until the root-mean-square gradient was less than 0.001 kcal/mol. The MD simulations were performed using the CHARMM 28B2 program in the isothermal–isobaric ensemble ($P = 1$ bar, $T = 298$ K). The particle mesh Ewald summation method[22] was used to treat the long-range electrostatic interactions. The bond lengths of water and each of the sugar molecules were constrained with the SHAKE algorithm.[23] The time step was 2.0 fs, and the non-bonded pair list was updated every 50 steps. The short-range non-bonded interactions were truncated with a 13 Å cutoff. The temperature and pressure of the system was regulated using the Langevin piston method in conjunction with Hoover's thermostat.[24] The system was gradually heated to 298 K for 40 ps and equilibrated for 400 ps at this temperature. The production MD trajectory with

one snapshot per 10 ps was collected for 10 ns. The hydrogen bonding and correlation functions were computed using the analysis facility (Corman and Correl modules) of the CHARMM program. The hydrogen bond was defined based on the geometric criteria of 3 Å distance and 120° angle. We used the IHYD command in the CORMAN module of CHARMM to calculate the hydration number of each of the sugar molecules. This method counts the number of solvent molecules within a predefined radius and includes normalization for the number of site atoms and time frames. Hydration number calculation was invoked by specifying a 3-Å hydration radius value to the CHARMM command.

All the dynamic simulations and trajectory analyses were performed on a computational Grid system, called MGrid (http://www.mgrid.or.kr), in order to process a large number of force-field calculations simultaneously. The MGrid system was designed to support remote execution, file transfers, and standard interface to legacy MPI (Message Passing Interface) applications to run successful MD simulations.

## 3. Results and discussion

### 3.1. Conformational and hydrational properties of trehalose

Figure 2 represents the calculated population density map for the dihedral angle distributions of trehalose. The diagonal symmetry of the map is a consequence of the conformational symmetry of this sugar. Trehalose showed its less-flexible conformation without any dihedral transition during 10-ns MD simulations. The most populated region lies on the line of symmetry at $\varphi$, $\psi$ values around (−44°, −44°), which are exactly correlated with the result from the experimental data on NMR solution conformation[25] (−44°, −44°) of trehalose. These suggest that the force fields and the computational methods employed are adequate to study the dynamic and hydrational aspects of the sugar.

The hydrational status of each disaccharide was characterized by radial-pair distribution functions (RDF) of water (Fig. 3). The RDFs around the oxygen atoms of each of the sugars were obtained with a well-defined first solvation shell with a density peak at 2.8 Å and a peak density of about 1.64 without significant differences between sugars (Fig. 3A). Since the RDF reflects the interaction with the solvent water molecules, each disaccharide was solvated by water with a similar quantity

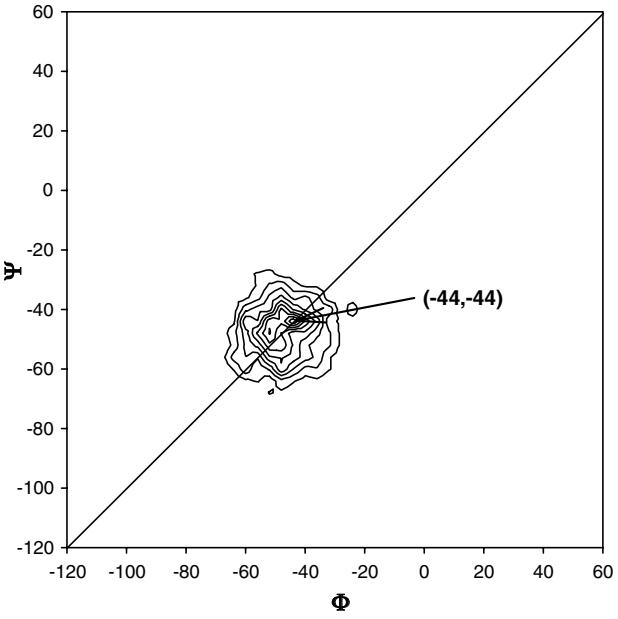


**Figure 2.** Population density map for the dihedral angle distributions of trehalose. The most populated $\phi$,$\psi$ space is located at (−44°, −44°), which correlates well with the experimental results from the NMR solution conformation. Trehalose showed its less-flexible conformation without any dihedral transition during 10-ns MD simulations.

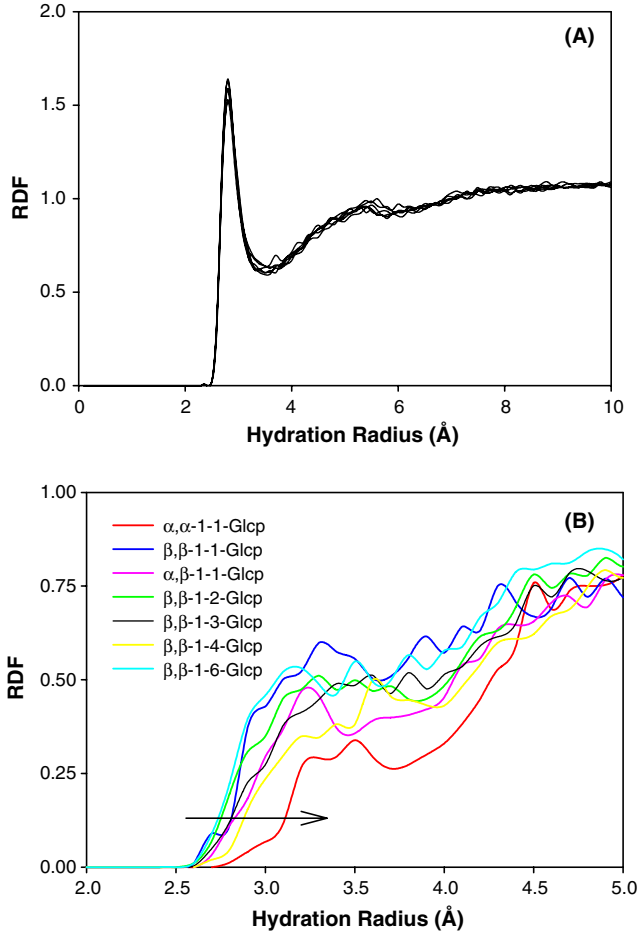


**Figure 3.** The radial distribution function (RDF) of water molecules around disaccharides. (A) RDF around all oxygen atoms of each disaccharide (B) RDF around glycosidic oxygen of **1**, **2**, **3**, **8**, **9**, **10**, and **11**. The RDF around the glycosidic oxygen of trehalose shows a clear outward shift of the first solvation peak compared to the other sugars.

during the MD simulations. However, water distribution patterns around the glycosidic oxygen are quite dissimilar to the patterns around all other oxygens (Fig. 3B). In particular, the RDF around the glycosidic oxygen of trehalose showed limited distribution of water over that of the other sugars. The RDFs of water for the glycosidic oxygen of three (1→1)-linked disaccharides were calculated. In all three cases, each characteristic first solvation peak at 2.8 Å was not observed. Instead, the RDF of each α-D-Glc*p*-(1→1)-α-D-Glc*p*, β-D-Glc*p*-(1→1)-β-D-Glc*p*, α-D-Glc*p*-(1→1)-β-D-Glc*p* (**1**, **2** and **3**) was found at 3.5, 3.3, and 3.2 Å with a peak density of 0.34, 0.60, and 0.47, respectively. This indicates that the glycosidic oxygens of the (1→1)-linked sugars, particularly trehalose, were not easily hydrated compared with the other oxygen atoms. Similarly, the RDFs of water around glycosidic oxygen of each α- or β-(1→2)-, (1→3)-, (1→4)-, (1→6)-linked disaccharide during MD simulations were analyzed. Peaks at 3.1, 3.2, 3.1, and 3.1 Å with a peak density of 0.43, 0.31, 0.22, and 0.41 were represented for the α-(1→2)-, (1→3)-, (1→4)-, (1→6)-linked Glc*p* (**4**, **5**, **6**, and **7**), respectively. In similar, each of the peaks at 3.1, 3.3, 3.2, and 3.1 Å with a peak density of 0.45, 0.44, 0.35, and 0.52 was for the β-(1→2)-, (1→3)-, (1→4)-, (1→6)-linked Glc*p* (**8**, **9**, **10**, and **11**), respectively (Fig. 3B). In all cases, the RDF peak of water around the glycosidic oxygen of trehalose showed the highest outward shift compared with that for the other sugars. Such an exclusive water distribution around the glycosidic oxygen was also confirmed by hydration number calculation (Table 1). The hydration number within first solvation shell from the RDF peak gives the quantitative information on the water distribution around each oxygen atom of the sugars. The average 0.153 of hydration numbers for the glycosidic oxygens are lower than those for the other oxygen atoms in all the disaccharides. In particular, the value of the glycosidic oxygen hydration for the trehalose was 0.028, which is much lower than all the other sugars except galactose and the mannose dimer.

These results mean that water molecules cannot be positioned in the vicinity of the glycosidic oxygen of (1→1)-linked disaccharides, particularly trehalose. This anisotropic distribution of water molecules nearby trehalose may determine unique biological property of trehalose. The (1→2)-, (1→3)-, (1→4)-, (1→6)-linked disaccharide was fully wrapped up in nearby water molecules less than 2.8 Å from the oxygen atoms of each sugar. But, water around trehalose was not distributed over all the sites of trehalose molecule. Figure 4 is the water distribution around each α-linked Glc*p* disaccharide for the most populated conformations during 10-ns MD simulations. The innermost water molecules were populated mainly around the 2-, 3-, and 4-OH of trehalose and not around other oxygen atoms. Trehalose is assumed to be laid on a relatively flat-shaped water shell and not on a round-shaped one. The disaccharide **4**, **5**, or **6** was fully wrapped up in nearby water molecules less than 2.8 Å from the heavy atoms of each sugar. Trehalose may replace the water molecules on a biological membrane through the direct interaction of an apolar face with the membrane head group,[7a] while the polar face makes contact with the expelled water molecules via hydrogen bonding. We think this anisotropic distribution of water molecules around the sugar

**Table 1.** Hydration number around each oxygen atom of the disaccharides

| Disaccharide | Oxygen atoms | | | | | |
|---|---|---|---|---|---|---|
| | O-1[a] | O-2 | O-3 | O-4 | O-5 | O-6 |
| **1** | 0.028 | 1.662 | 1.561 | 1.535 | 0.239 | 1.810 |
| **2** | 0.252 | 1.600 | 1.601 | 1.508 | 0.234 | 1.840 |
| **3** | 0.154 | 1.652 | 1.525 | 1.499 | 0.246 | 1.707 |
| **4** | 0.254 | 1.713 | 1.585 | 1.464 | 0.281 | 1.789 |
| **5** | 0.125 | 1.505 | 1.509 | 1.401 | 0.275 | 1.746 |
| **6** | 0.096 | 1.579 | 1.419 | 1.546 | 0.280 | 1.660 |
| **7** | 0.204 | 1.673 | 1.563 | 1.453 | 0.238 | 1.809 |
| **8** | 0.245 | 1.562 | 1.522 | 1.456 | 0.333 | 1.792 |
| **9** | 0.180 | 1.537 | 1.610 | 1.368 | 0.278 | 1.760 |
| **10** | 0.119 | 1.570 | 1.427 | 1.484 | 0.255 | 1.700 |
| **11** | 0.306 | 1.612 | 1.561 | 1.428 | 0.339 | 1.829 |
| **12** | 0.028 | 1.651 | 1.533 | 1.327 | 0.278 | 1.827 |
| **13** | 0.002 | 1.441 | 1.587 | 1.508 | 0.289 | 1.805 |
| Average | 0.153 | 1.597 | 1.539 | 1.460 | 0.274 | 1.775 |

[a] All the α,α-(1→1)-linked disaccharides showed lower hydration numbers around glycosidic oxygen O-1.

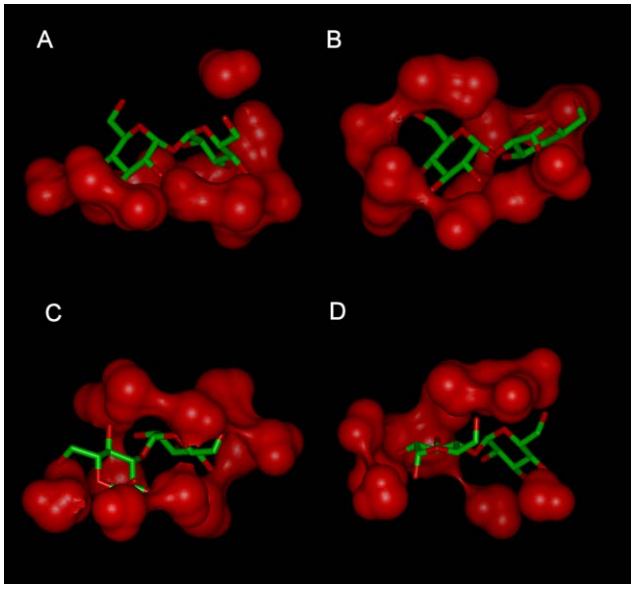


**Figure 4.** Schematic representations of water structure around the α-linked disaccharides, **1** (A), **4** (B), **5** (C), and **6** (D). The solvent-accessible surface area of water molecules less than 2.8 Å from the heavy atoms of each disaccharide was rendered as a Connolly surface in red color. Only α,α-(1→1)-linked trehalose showed anisotropic water distribution among the other (1→2)-, (1→3)-, or (1→4)-linked sugars.

is the decisive factor in determining the conformation and hence the biological function of trehalose compared with the other sugars. To discuss the quantitative effect of anisotropic hydration on the conformation of trehalose, we analyzed the collected motions and the hydrogen-bonding patterns of each glycosidic linkage.

### 3.2. Molecular motion of the sugars and water interaction

Figure 5 shows the time-correlation functions of collected motions for the glycosidic linkage of each sugar. The time-correlation function of the motion is defined by the following formula $Q(t) = X_1(t) - X_2(t)$, where $X(t)$ is the time function of the atomic position of carbon atoms linked to the glycosidic oxygen of residue **1** ($X_1$) and residue **2** ($X_2$) of each disaccharide. The correlation function provides a measure of the long-lived scale tumbling motions of the sugars overall. One can obtain valuable information on the dynamic properties of molecules from the decay pattern of the correlation functions.[26] In the series of α-linked disaccharides, trehalose showed the lowest motional changes of the glycosidic linkage during MD simulations. The lifetimes for the internal motions of each glycosidic linkage were 4.74 ns for **1**, 3.13 ns for **2**, 3.16 ns for **3**, 3.00 ns for **4**, 1.75 ns for **5**, 2.89 ns for **6**, and 2.61 ns for **7**. Therefore, the dynamic motion about the glycosidic linkage occurs much more slowly in trehalose than in the other sugars in aqueous solution. The dynamic conformation of the carbohydrate is readily affected by the solvent interaction.[27] Thus, the reason for such a conformational behavior of trehalose can be established based on the interaction with water molecules.

Interestingly, we discovered that the glycosidic oxygens of three α,α-(1→1)-linked disaccharides (**1**, **12** and **13**) were practically not hydrated by water molecules compared with the other sugars. However, the hydration numbers around all the other oxygen atoms of the various disaccharides were not much different. The glycosidic linkage is the most important factor to change the whole molecular conformation. The hydration number, 0.028, for the glycosidic oxygen of trehalose was just 11% of the number of the α,α-(1→2)-linked glucose dimer (0.254) and 18% of the average value (0.153) for the other disaccharides (Table 1). That means that water molecules cannot dynamically perturb the glycosidic oxygen of α,α-(1→1)-linked sugars unlike any other (1→2)-, (1→3)-, (1→4)-, (1→6)-glycosidic linkage. For that reason, the trehalose molecule is able to maintain its rigid conformation in contrast to the other linkage-typed sugars even in a water environment.

### 3.3. Rotational and translational motions of water around sugars

The relationship between the conformational rigidity of trehalose and the vibrational motion of water molecules was characterized by the rotational correlation times (Fig. 6) and translational diffusion coefficients of water molecules (Table 2). To characterize water structures and to follow the dynamics of solutes involving water, it is necessary to examine the motions of the solvents in detail. Hence we calculated from the MD trajectory files the rotational correlation times[26b,28] of water molecules for three rotational motions: wagging, twisting, and rocking ($\tau_{wag}$, $\tau_{twist}$, $\tau_{rock}$). The rotational correlation time was calculated by fitting the exponentional

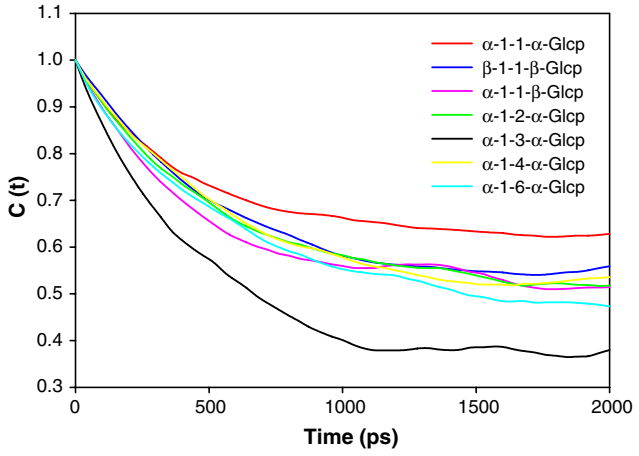


**Figure 5.** Autocorrelation of the existence function for the collected motion of each glycosidic linkage. The motion was defined as any atomic displacement of glycosidic linkage vector, C-1–O-1–C-X pair, for the *x*-,*y*-, and *z*-directions during MD simulations.

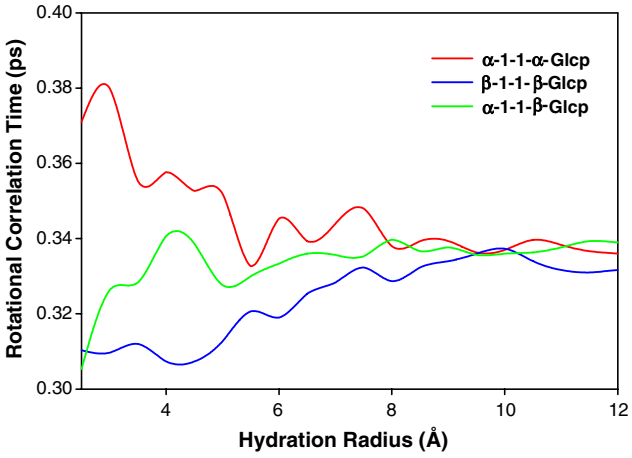


**Figure 6.** Rotational correlation times for TIP3P water in the vicinity of a α-D-Glc*p*-(1→1)-α-D-Glc*p*, β-D-Glc*p*-(1→1)-β-D-Glc*p*, and α-D-Glc*p*-(1→1)-β-D-Glc*p*. The average rotational correlation time of the three motions of $\tau$ for authentic trehalose was larger than those of β-D-Glc*p*-(1→1)-β-D-Glc*p* or α-D-Glc*p*-(1→1)-β-D-Glc*p*. These results indicate that trehalose enforces the lowest rotational degree of freedom on the nearby water molecules than do the other two sugars.

**Table 2.** Translational diffusion coefficients of water around 3 Å distance of oxygen atoms of each disaccharide[a]

| Disaccharides | Diffusion coefficients ($cm^2/s$) |
|---|---|
| **1** | $(0.59 \pm 0.008) \times 10^{-5}$ |
| **2** | $(0.71 \pm 0.009) \times 10^{-5}$ |
| **3** | $(0.67 \pm 0.007) \times 10^{-5}$ |
| **4** | $(0.61 \pm 0.008) \times 10^{-5}$ |
| **5** | $(0.75 \pm 0.008) \times 10^{-5}$ |
| **6** | $(0.61 \pm 0.009) \times 10^{-5}$ |
| **7** | $(0.71 \pm 0.008) \times 10^{-5}$ |
| **8** | $(0.75 \pm 0.009) \times 10^{-5}$ |
| **9** | $(0.67 \pm 0.010) \times 10^{-5}$ |
| **10** | $(0.63 \pm 0.010) \times 10^{-5}$ |
| **11** | $(0.68 \pm 0.008) \times 10^{-5}$ |
| **12** | $(1.96 \pm 0.010) \times 10^{-5}$ |
| **13** | $(1.82 \pm 0.020) \times 10^{-5}$ |

[a] The lowest value of water around trehalose means that trehalose is most effectively decreasing the mobility of the neighboring water molecules in comparison with the other sugars.

decay component of the corresponding time correlation function $C(t)$ to an exponentional function of the form $C(t) = A \cdot e^{-t/\tau}$, where $\tau$ is the correlation time. The averaged value of $\tau_{wag}$, $\tau_{twist}$, and $\tau_{rock}$ within the first solvation shell was 0.38 ps for α-D-Glc*p*-(1→1)-α-D-Glc*p*, 0.31 ps for β-D-Glc*p*-(1→1)-β-D-Glc*p*, and 0.32 ps for α-D-Glc*p*-(1→1)-β-D-Glc*p*, respectively. The average values of the three motions of $\tau$ for trehalose were larger than those of other (1→1)-linked glucose dimers in any distance range of solute–solvent (Fig. 6). The larger $\tau$ value of water for trehalose indicates that water around trehalose rotates less freely compared to the cases of the other sugars. This observation is well correlated with the translational diffusion of water around each sugar (Table 2). The coefficient around trehalose was $0.59 \times 10^{-5}$ $cm^2/s$, which is much lower than the average value of $0.86 \times 10^{-5}$ $cm^2/s$ for the 13 different sugars. The translational diffusion of trehalose solution has recently been determined experimentally as $\sim 0.3 \times 10^{-5}$ $cm^2/s$ by Magazù et al.[29] and $\sim 0.4 \times 10^{-5}$ $cm^2/s$ by Rampp et al.[30] for a 10% (w/w) solution. The calculated translational diffusion from the MD simulations determined by other groups at $\sim 0.51 \times 10^{-5}$ $cm^2/s$ is also very similar to that of our value of $0.59 \times 10^{-5}$ $cm^2/s$. Engelsen and Pérez[18] discovered that the calculated translational diffusion of trehalose was very similar to that of sucrose, while the calculated rotational diffusion is much slower. Pablo and co-workers[17] also found that the hydration number of the trehalose solution was much larger than that of the sucrose solution. These results are finely correlated with our computational results. Our findings indicate that trehalose restricted the dynamics of water molecules by strong hydrogen bonding to water. The translational and rotational time data suggest that water molecules around the trehalose were positionally and orientationally restricted to form stable hydrogen bonds in all directions.

### 3.4. Hydrogen-bond network of the sugars with water molecules

The anisotropic hydration and the less-flexible conformation of trehalose are expected to result in a stable solvent interaction via formation of long-lived hydrogen bonds. The averaged number of hydrogen bonds between each disaccharide and water molecules was, for example, 8.7 for trehalose, 8.5 for maltose, and 8.7 for the mannose dimer. Other disaccharides also formed the same hydrogen bonds with water as those of trehalose. Although the hydrogen bond number gave an average view on the accessibility of sugar molecules to water, it could not be considered as a valid measure of the residence dynamics of water molecules in specific hydration sites of the sugars. However, the long-lived hydrogen bond formation for the disaccharides with water was a good index reflecting the strength of the sugar–water interactions. We defined the long-lived hydrogen bond as a hydrogen bond with a lifetime longer than 20 ps, because the lifetime of pure water was known to be in the 1–10 ps range.[31] Trehalose made an average of 2.8 of long-lived hydrogen bonds with water, which is a much larger number than the average number of hydrogen bonds for the other 12 sugars. However, the long-lived hydrogen bonds of α-D-Gal*p*-(1→1)-α-D-Gal*p* or α-D-Man*p*-(1→1)-α-D-Man*p* were much lower than the average though their anisotropic hydration as in trehalose. Thus axial hydroxyl groups on the galactose (4-OH) and mannose (2-OH) seem to disturb the formation of stable hydrogen bonds with water. The axial groups in general have lower accessible surfaces than equatorial groups, and they are closer to the molecular center of mass, giving less opportunity for forming hydrogen bonds in crystal structures.[32] The number of long-lived water bridges were also highest in the case of trehalose. Water bridges are recurrent motifs in macromolecular hydration. Trehalose made 50 long-lived water bridges during 10-ns MD simulations, which were 1.7-fold higher than the average value of the other sugars. This strong rearrangement of water caused by trehalose was confirmed in terms of nonbonding interactions between water molecules. The columbic interaction energy between water molecules within the first solvation shell of trehalose was −13.16 kcal/mol, which is much lower than the average value of −11.52 kcal/mol for all the other sugars. It is highly noticeable because the intermolecular energy between bulk water was not different in any sugar type (data not shown). That means that the water motion around trehalose was lowered as a result of the extensive hydrogen-bond network rearrangement dynamics.[33] The hydration number, hydrogen-bonding patterns, and intermolecular coulombic energy of water for each disaccharide are summarized in Table 3.

**Table 3.** Hydrational characteristics of 13 different disaccharides

| Disaccharide | $N_{HD\_O1}$[a] | $N_{HB}$[b] | $N_{HB\_Long}$[c] | $N_{bridge}$[d] | $\Delta E_{water\_shell}$[e] | $N_{water\_shell}$[f] | $N_{water\_total}$[g] |
|---|---|---|---|---|---|---|---|
| **1** | 0.028 | 8.7 | 2.8 | 50 | −13.16 | 12.79 | 534 |
| **2** | 0.252 | 8.8 | 2.2 | 36 | −11.64 | 12.64 | 536 |
| **3** | 0.154 | 8.6 | 2.2 | 28 | −10.30 | 12.18 | 536 |
| **4** | 0.254 | 8.2 | 1.8 | 41 | −12.18 | 12.51 | 538 |
| **5** | 0.125 | 8.4 | 2.5 | 30 | −11.26 | 12.03 | 535 |
| **6** | 0.096 | 8.5 | 2.3 | 35 | −11.08 | 12.03 | 533 |
| **7** | 0.204 | 8.8 | 2.1 | 30 | −11.96 | 12.43 | 537 |
| **8** | 0.245 | 8.6 | 2.3 | 38 | −11.54 | 12.52 | 536 |
| **9** | 0.180 | 8.5 | 2.2 | 30 | −11.92 | 12.31 | 537 |
| **10** | 0.119 | 8.3 | 2.1 | 39 | −11.27 | 12.31 | 534 |
| **11** | 0.306 | 8.9 | 2.5 | 26 | −11.48 | 12.60 | 537 |
| **12** | 0.028 | 8.4 | 1.4 | 2 | −10.96 | 12.12 | 540 |
| **13** | 0.002 | 8.7 | 1.2 | 3 | −10.99 | 12.31 | 537 |
| Average | 0.153 | 8.6 | 2.1 | 30 | −11.52 | 12.37 | 536.2 |

[a] $N_{HD\_O1}$ Hydration number around the glycosidic oxygen.
[b] $N_{HB}$ Averaged number of hydrogen bonds between each disaccharide and water molecules.
[c] $N_{HB\_Long}$ Averaged number of long-lived hydrogen bonds between each disaccharide and water molecules.
[d] $N_{bridge}$ Total number of long-lived water bridges.
[e] $\Delta E_{water\_shell}$ Coulombic intermolecular energy (kJ/mol) between water molecules within the first solvation shell. The first solvation shell is defined as the range of 3 Å distance of oxygen atoms of each disaccharide.
[f] $N_{water\_shell}$ Averaged number of water molecules within the first solvation shell.
[g] $N_{water\_total}$ Total number of water molecules in each simulation system.

## 4. Conclusions

The overall results indicate that water readily interacts with sugars through instant hydrogen-bonding exchange without any specificity. However, at the same time, water molecules are able to form long-lived interactions with the sugars, depending on the anisotropic distribution around the sugar geometry. Water molecules are known to play an important role in the regulation of biological processes or reactivities.[34] Osmotic pressure or hydrational equilibrium is affected by changes in the activity of the surrounding water. Our findings provide a molecular interpretation of the hypothesis that α-D-Glc*p*-(1→1)-α-D-Glc*p* (trehalose) can regulate and protect the organism from osmotic pressure changes, freezing, or extreme desiccation through the control of water activity by the formation of long-lived hydrogen bonds. MD simulation results showed that such a stable solvent interaction of trehalose was due to rigid glycosidic linkage motion by anisotropic water distribution. This theoretical finding on the solvent interaction of sugars described herein could be extended to various other glycosidic linkages in the field of carbohydrate engineering and could also be applied to the molecular design of novel osmo- or cryoprotectants using carbohydrates. We suggest that organic synthesis of sugar-type 'dynamic enhancers' or 'dynamic reducers' for the solvent is highly desirable with modification of the glycosidic linkage or hydroxyl groups.

## Acknowledgements

This study was supported by a grant of the *e*-Science Project of KISTI (Korea Institute of Science and Technology Information) in MOST (Ministry of Science and Technology).

## References

1. (a) Elbein, A. D.; Pan, Y. T.; Pastuszak, I.; Carroll, D. *Glycobiology* **2003**, *13*, 17R–27R; (b) Crowe, J.; Crowe, L.; Chapman, D. *Science* **1984**, *223*, 209–217.
2. (a) Higashiyama, T. *Pure Appl. Chem.* **2002**, *74*, 1263–1269; (b) Crowe, J.; Carpenter, J.; Crowe, L. *Annu. Rev. Physiol.* **1998**, *60*, 73–103; (c) Sussich, F.; Skopec, C.; Brady, J.; Cesàro, A. *Carbohydr. Res.* **2001**, *334*, 165–176.
3. (a) Cabib, E.; Leloir, L. *J. Biol. Chem.* **1958**, *231*, 259–275; (b) Roth, R.; Sussmann, M. *Biochim. Biophys. Acta* **1966**, *122*, 225–231.
4. (a) Maruta, K.; Hattori, K.; Nakada, T.; Kubota, M.; Sugimoto, T.; Kurimoto, M. *Biosci. Biotechnol. Biochem.* **1996**, *60*, 717–720; (b) Maruta, K.; Hattori, K.; Nakada, T.; Kubota, M.; Sugimoto, T.; Kurimoto, M. *Biochim. Biophys. Acta* **1996**, *1289*, 10–13.
5. (a) Miller, K. J.; Wood, J. M. *Annu. Rev. Microbiol.* **1996**, *50*, 101–136; (b) D'Souza-Ault, M. R.; Smith, L. T.; Smith, G. M. *Appl. Environ. Microbiol.* **1993**, *59*, 473–478; (c) Soto, M. J.; Lepek, V.; Olivares, J.; Toro, N. *Mol. Plant-Microbe Interact.* **1993**, *6*, 11–14.
6. Crowe, L. M.; Reid, D. S.; Crowe, J. H. *Biophys. J.* **1996**, *71*, 2087–2093.
7. (a) Villarreal, M. A.; Diaz, S. B.; Disalvo, A.; Montich, G. *Langmuir* **2004**, *20*, 7844–7851; (b) Patist, A.; Zoerb, H. *Coll. Sur. B: Biointerfaces* **2005**, *40*, 107–113; (c) Branca, C.; Magazù, V.; Maisano, G.; Migliardo, F.; Soper, A. K. *Appl. Phys. A* **2002**, *74*, S450–S451.
8. Green, J. L.; Angell, C. A. *J. Phys. Chem.* **1989**, *93*, 2880–2882.
9. (a) Dowd, M. K.; Reilly, P. J.; French, A. D. *J. Comp. Chem.* **1992**, *12*, 102–114; (b) Kuttel, M. M.; Naidoo, K. J. *Carbohyr. Res.* **2005**, *340*, 875–879.

10. Liu, Q.; Schmidt, R. K.; Teo, B.; Karplus, P. A.; Brady, J. W. *J. Am. Chem. Soc.* **1997**, *119*, 7851–7862.
11. Bush, C. A.; Pastor, M. M.; Imberty, A. *Annu. Rev. Biophys. Biomol. Struct.* **1999**, *28*, 269–293.
12. Iannilli, E.; Tettamanti, E.; Galantini, L.; Magazù, S. *J. Phys. Chem. B* **2001**, *105*, 12143–12149.
13. Kawai, H.; Sakurai, M.; Inoue, Y.; Chujo, R.; Kobayashi, S. *Cryobiology* **1992**, *29*, 599–606.
14. Magazù, S.; Migliardo, P.; Musolino, A. M.; Sciortino, M. T. *J. Phys. Chem. B* **1997**, *101*, 2348–2351.
15. Elias, M. E.; Elias, A. M. *J. Mol. Liq.* **1999**, *83*, 303–307.
16. Russo, D.; Hura, G.; Head-Gordon, T. *Biophys. J.* **2004**, *86*, 1852–1862.
17. Ekdawi-Sever, N. C.; Conrad, P. B.; de Pablo, J. J. *J. Phys. Chem. A* **2001**, *105*, 734–742.
18. Engelsen, S. B.; Pérez, S. *J. Phys. Chem. B* **2000**, *104*, 9301–9311.
19. Brooks, B. R.; Bruccoleri, R. E.; Olafson, B. D.; States, D. J.; Swaminathan, S.; Karplus, M. *J. Comput. Chem.* **1983**, *4*, 187–217.
20. Naidoo, K. J.; Kuttel, M. *J. Comput. Chem.* **2001**, *22*, 445–456.
21. Jorgensen, W. L. *J. Chem. Phys.* **1982**, *77*, 4156–4163.
22. Darden, T.; York, D.; Pedersen, L. *J. Chem. Phys.* **1993**, *98*, 10089–10092.
23. Ryckaert, J. P.; Ciccotti, G.; Berendsen, H. J. C. *J. Comput. Phys.* **1977**, *23*, 327–341.
24. Feller, S. E.; Zhang, Y.; Pastor, R. W.; Brooks, B. R. *J. Chem. Phys.* **1995**, *103*, 4613–4621.
25. (a) Batta, G.; Kover, K. E.; Gervay, J.; Hornyak, M.; Roberts, G. M. *J. Am. Chem. Soc.* **1997**, *119*, 1336–1345; (b) Cheetham, N. W. H.; Dasgupta, P.; Ball, G. E. *Carbohydr. Res.* **2003**, *338*, 955–962.
26. (a) Best, R. B.; Jackson, G. E.; Naidoo, K. J. *J. Phys. Chem. B* **2001**, *105*, 4742–4751; (b) Choi, Y.; Jung, S. *Carbohydr. Res.* **2005**, *340*, 2550–2557.
27. Kirschner, K. N.; Woods, R. J. *Proc. Natl. Acad. Sci. U.S.A.* **2001**, *98*, 10541–10545.
28. (a) Johannesson, H.; Halle, B. *J. Am. Chem. Soc.* **1998**, *120*, 6859–6870; (b) Wallqvist, A.; Berne, B. J. *J. Phys. Chem.* **1993**, *97*, 13841–13851.
29. Magazù, S.; Maisano, G.; Middendorf, H. D.; Migliardo, P.; Musolino, A. M.; Villari, V. *J. Phys. Chem.* **1998**, *102*, 2060–2063.
30. Rampp, M.; Buttersack, C.; Ludemann, H. D. *Carbohydr. Res.* **2000**, *328*, 561–572.
31. Keutsch, F. N.; Saykally, R. J. *Proc. Natl. Acad. Sci. U.S.A.* **2001**, *98*, 10533–10540.
32. Bonnet, A.; Chisholm, J.; Motherwell, W. D.; Jones, W. *Cryst. Eng. Commun.* **2005**, *7*, 71–75.
33. Matsumoto, M.; Saito, S.; Ohmine, I. *Nature* **2002**, *416*, 409–413.
34. Eisenberg, D.; McLachlan, A. D. *Nature* **1986**, *319*, 199–203.